REPORT DOCUMENTATION PAGE

Form Approved
OMB No. 0704-0188

1. AGENCY USE ONLY (Leave blank)	2. REPORT DATE	3. REPORT TYPE AND DATES COVERED
	September 21, 1994	Technical

4. TITLE AND SUBTITLE
THE DYNAMICS OF FORMATION AND EVAPORATION OF MIXED ALKALI HALIDE NANOCRYSTALS: A CASE OF COMPARABLE LATTICE ENERGIES

5. FUNDING NUMBERS
GRANT N00014-89-J-1350
R&T Code 4131015
Ronald A. De Marco

6. AUTHOR(S)
Temer S. Ahmadi and M. A. El-Sayed

7. PERFORMING ORGANIZATION NAME(S) AND ADDRESS(ES)
Regents of the University of California
University of California
405 Hilgard Avenue
Los Angeles, CA 90024

8. PERFORMING ORGANIZATION REPORT NUMBER
79

9. SPONSORING/MONITORING AGENCY NAME(S) AND ADDRESS(ES)
Office of Naval Research N00014
Chemistry Branch
Arlington, VA 22217

10. SPONSORING/MONITORING AGENCY REPORT NUMBER

11. SUPPLEMENTARY NOTES

12a. DISTRIBUTION AVAILABILITY STATEMENT
This document has been approved for public release and sale; distribution of this document is unlimited.

12b. DISTRIBUTION CODE

13. ABSTRACT (Maximum 200 words)

The relative intensity distribution of the $[Rb_nK_{14-n}I_{13}]^+$ mixed nanocrystals containing a "magic" number of 14 metal cations and 13 iodide anions is examined. These nanocrystals were generated through sputtering of mixed RbI / KI solids using fast atom bombardment, and analyzed by use of a double-focusing sector-field mass spectrometer. The relative intensities of the observed peaks is found to have a 'bimodal' distribution with a maximum near n =7. This observation is explained by assuming: (a) a rate of formation that is proportional to the number of isomers that can be formed for each mixed nanocrystal, and (b) a rate of dissociation that is insensitive to the composition of the mixed nanocrystal. The later assumption leads to the conclusion that the internal energies of these mixed nanocrystals are similar and independent of their composition. This conclusion is supported by the results of Monte Carlo simulation annealing as well as by the similarity of the known lattice energies of KI and RbI bulk crystals.

14. SUBJECT TERMS	15. NUMBER OF PAGES 22
	16. PRICE CODE

17. SECURITY CLASSIFICATION OF REPORT	18. SECURITY CLASSIFICATION OF THIS PAGE	19. SECURITY CLASSIFICATION OF ABSTRACT	20. LIMITATION OF ABSTRACT
UNCLASSIFIED	UNCLASSIFIED	UNCLASSIFIED	

OFFICE OF NAVAL RESEARCH

GRANT N00014-89-J-1350
Ronald A. DeMarco

R&T CODE 4131015

Technical Report N. 79

THE DYNAMICS OF FORMATION AND EVAPORATION OF MIXED ALKALI HALIDE NANOCRYSTALS: A CASE OF COMPARABLE LATTICE ENERGIES

by

Temer S. Ahmadi and Mostafa A. El-Sayed

Accepted for Publication

in the

Journal of Physical Chemistry

Department of Chemistry and Biochemistry
University of California, Los Angeles
Los Angeles, CA 90024-1569

September 27, 1994

The Dynamics of Formation and Evaporation of Mixed Alkali Halide Nanocrystals: A Case of Comparable Lattice Energies

Temer S. Ahmadi and Mostafa A. El-Sayed
Department of Chemistry and Biochemistry
University of California, Los Angeles, California 90024

Abstract

The relative intensity distribution of the $[Rb_nK_{14-n}I_{13}]^+$ mixed nanocrystals containing a "magic" number of 14 metal cations and 13 iodide anions is examined. These nanocrystals were generated through sputtering of mixed RbI / KI solids using fast atom bombardment, and analyzed by use of a double-focusing sector-field mass spectrometer. The relative intensities of the observed peaks is found to have a 'bimodal' distribution with a maximum near n = 7. This observation is explained by assuming: (a) a rate of formation that is proportional to the number of

isomers that can be formed for each mixed nanocrystal, and (b) a rate of dissociation that is insensitive to the composition of the mixed nanocrystal. The later assumption leads to the conclusion that the internal energies of these mixed nanocrystals are similar and independent of their composition. This conclusion is supported by the results of Monte Carlo simulation annealing as well as by the similarity of the known lattice energies of KI and RbI bulk crystals.

I. Introduction

Because of their elementary electronic properties, the alkali halide clusters have been extensively studied both theoretically and experimentally[1-32]. In 1981, Campana[16] et. al. used Xenon-ion bombardment of CsI to generate cluster ions of the type $[M_nX_{n-1}]^+$ (for n values up to 70) which were detected by a secondary-ion mass spectrometer. They noted an irregularity in the relative abundance of the cluster-ions, indicating small deviations from the expected[16,31] monotonic decrease in ion intensity as the cluster size increased (since larger clusters require higher number of collisions for their nucleation). These deviations or "local maxima" occur at n= 14, 23, 38, and 63 . These n values are called the "magic numbers" and are attributed to the formation of relatively stable[27,31] 3X3X3, 3X3X5, 3X5X5, and 5X5X5 cuboid structures. This relative stability diminishes the rate of their decomposition prior to their detection, thus, allowing them to have relatively stronger peak intensities in the mass spectrum.

A direct determination of the structure of these cluster-ions has not been possible; however, Martin[33] used total energy calculations to determine the most stable structures of $[Na_nCl_{n-1}]^+$ cluster-ions (n= 1-18). For n =14, one of the "magic numbers", he found a 3X3X3 face-centered-cubic lattice structure. Calculations by others have confirmed Martin's work[3,15]. The mass spectra of all of the alkali halides have the same "magic numbers", indicating a face-centered-cubic (fcc) structure for all of them irrespective of their bulk crystalline structures, e.g. bulk NaCl, NaI, NaF, KF, KI, and KCl crystallize into fcc structures, whereas bulk CsCl and CsI form a body-centered-cubic (bcc) lattice[10,39].

The structure and relative yield of small mixed alkali halide clusters have also been examined[12, 29, 39]. Diefenbach and Martin[12] found that cluster-ions of mixed alkali halides are stable even for compositions that do not form solid solutions in the condensed phase (e.g. NaI and CsI). Using the polarizable-ion model , they calculated the total energies and the corresponding geometries of these clusters. It was found that mixed clusters with ions of comparable sizes(e.g. Rb^+, Cs^+) give the most stable structures[12].

In an effort to examine the effect of defects on the formation and stability of nanocrystals, we have previously[36] studied the addition of an AgI molecule to the Ag_n^+ cluster-ion. The structure of the mixed clusters were deduced from the observed evaporation dynamics and the interactions resulting from the adhesion of the AgI molecules to the metallic clusters. In the present work, we experimentally determined the intensity distribution of mixed alkali halide nanocrystals as RbI molecules replace KI molecules in the nanocrystal cation of the type $[Rb_nK_{14-n}I_{13}]^+$

with n = 0, 1, ..., 14. We found that the observed intensity distribution is largely determined by the number of configurations (isomers) that different mixed nanocrystals can have. A simple kinetic model shows that this situation can arise if the stability (internal energy) of the different mixed nanocrystals is independent of their exact composition, i.e. independent of the value of n within these mixed nanocrystals. A theoretical calculation of the internal energy of these nanocrystals using Monte Carlo technique indeed support this assumption.

II. Experimental

The mass spectra of the mixed alkali halide nanocrystals of the type $[Rb_nK_{14-n}I_{13}]^+$ (n=0-14) were obtained by the use of a VG Analytical ZAB-SE* mass spectrometer (reverse geometry) fitted with a fast atom (Xe) bombardment gun. The details of the experimental have been reported previously[21]. Briefly, a non-saturated solution of equal molar ratio of each of RbI and KI was prepared in distilled water and was placed on the probe tip. The water was dried off leaving mixed-crystals on the tip[32]. Cluster-ions were prepared by the bombardment of the mixed-crystals by an 8 keV Xe atom gun. An acceleration voltage of 8 keV was applied to the cations to extract them from the source. The accelerating ions were analyzed with the magnetic sector in conjunction with the electric sector, and detected by a conversion dynode followed by an electron multiplier[21].

The relative intensity of a certain mixed nanocrystal in the distribution is determined by the ratio of its intensity to the sum of the intensities of the fifteen peaks observed for all of the nanocrystals from

n = 0 to n = 14. The pressure in the acceleration region was kept at ~ 5 $X10^{-6}$ Torr and in the analyzer at ~5 $X10^{-8}$ Torr. We collected three sets of 200 scans on three different days to ensure reproducibility. A typical spectrum is given in Figure 1, where the peaks corresponding to n = 0 to n=14 of the $[Rb_nK_{14-n}I_{13}]^+$ nanocrystals are marked.

III. Results

We used fast atom bombardment mass spectrometry to generate the mixed cluster-ions of the type $[Rb_nK_{14-n}I_{13}]^+$ (n=0-14). A mass spectrum of these cluster-ions is shown in figure 1. Using this spectrum, we calculated the observed intensity distribution for these clusters by calculating fraction (F_k) of ions observed for the kth mixed cluster-ion, having an intensity I_k in the mass spectrum by use of the following equation:

$$F_k = (I_k / \sum_{n=0}^{14} I_n) X 100 \quad \text{----------} \quad (1)$$

A 'bimodal' distribution for the probability distribution of these cluster-ions centered near n = 7 was obtained and is shown in Fig. 2. These results suggests that more nanocrystal ions are detected with near comparable number of RbI and KI molecules. These are also the nanocrystals with the maximum number of configurations (isomers) that one can write for the nanocrystals made of 3X3X3 lattices of atomic species. For a nanocrystal $[Rb_nK_{14-n}I_{13}]^+$, this number W_k is given by :

$$W_k = (14! / k! (14-k)!) \quad \text{----------} \quad (2)$$

The fraction P_k is the ratio of the number of possible configurations (isomers) for any nanocrystal k with k Rb to the total number of possible configurations for all of the nanocrystals, i.e.

$$P_k = (W_k / \sum_{n=0}^{14} W_n) \quad \text{----------} \quad (3)$$

Figure 3 shows a plot of the fraction P_k as a function of n. The maximum of this distribution is at n = 7.

Below, we discuss a kinetic model that might be responsible for the formation of these mixed nanocrystals by the sputtering technique. We then find out the conditions under which the kinetic model lead to a distribution that is controlled by the number of isomers that each of these mixed nanocrystals can have.

IV. Discussion

A. Simple Kinetic Model for Mixed Nanocrystal Formation

Let us assume that $[Rb_nK_{14-n}I_{13}]^+$ nanocrystals are formed rapidly from the collisions between the atoms and ions which are produced initially through sputtering of the solid surface. The rapid formation of these nanocrystals is followed by cooling processes resulting from the different channels of evaporation (unimolecular decompositions). In this simplified model, we may write the number of ions (N_k) observed for a certain cluster k as

$$N_k = N_k^{formed} - N_k^{decomposed} \quad \text{----------} \quad (4)$$

A certain cluster k can be formed by nucleation resulting from the many sticky collisions between a certain cation and the dipolar KI and RbI molecules. It can also be formed from the evaporative cooling of a less stable nanocrystal that has one or two molecules of KI and/or RbI beyond the magic number (e. g. $[Rb_{n+1}K_{15-n}I_{14}]^+$, $[Rb_{n+2}K_{16-n}I_{15}]^+$, where n = 0-14).

B. Formation of Nanocrystals Through Nucleation

The experiments of Ens[31] et. al. have clearly shown that the intensity of mass peaks decrease exponentially with size if the clusters are detected immediately after their formation without giving them time to undergo evaporation. This suggests that sputtering atomizes the solid, and then the atoms nucleate to form the different nanocrystals. The larger the number of collisions required for the formation of a nanocrystal, the smaller is its probability of formation. When nanocrystals undergo evaporative cooling prior to their detection, the naoncrystals with one or two alkali halide molecules more than the ones with magic numbers evaporate[21, 32] their excess molecules to attain the stable structure of the magic ones.

It is reasonable to assume that the nanocrystals under study are formed by the heterogeneous nucleation in which a metal cation(K^+ or Rb^+) seeds the nucleation of nanocrystal by attracting KI and RbI molecules. This would require a certain number of collisions , Z_n , to form a

nanocrystal of a fixed composition and arrangement (i.e. a certain isomer). If one assumes that a nanocrystal of a certain composition(a fixed value of n, say k) requires Z_k number of collisions, then the number of nanocrystal ions formed from the nucleation process, N_k^{form}, is written as

$$N_k^{form} \approx N_k^{isom} e^{-Z_k C_k} \quad \text{----------} \quad (5)$$

If the collisions are all sticky, one can assume that the number of collisions required to form any one of the configurations of any of the fifteen nanocrystals is the same (i.e. $C_n Z_n$ is the same for any isomer having a value of n). This allows us to write equation (5) as

$$N_k^{form} = K\, N_k^{isom} \quad \text{----------} \quad (6)$$

where the constant K is equal to $K' e^{-Z_k C_k}$.

If the detection time is shorter than evaporation time from these nanocrystals as in the Ens[13] et. al. experiment, and if the sensitivity of the detector is similar for all the mixed nanocrystal, then the predicted relative peak intensity is given by

$$N_k^{form} = (N_k^{isom} / \sum_{n=0}^{14} N_n) \text{---------} \quad (7)$$

As shown in eq. (3), the number of configurations (isomers) that can be written for the various compositions should have a maximum value for n=7. This is in reasonable agreement with the observation in Fig. 2. However, under our experimental condition, it was shown previously that evaporation indeed takes place. Thus we need to include the effect of such processes on the nanocrystal distribution. This is done in section C.

C. Inclusion of Evaporative Cooling

Incorporation of evaporative cooling changes the kinetic scheme by introducing additional sources of formation as well as a decay route for each nanocrystal. These processes give rise to the observed large relative intensities for nanocrystals with magic numbers. Our previous studies[1] on $[Cs_nI_{n-1}]^+$, carried out on the same instrument we are presently using, have shown that larger clusters undergo evaporation of CsI and $(CsI)_2$ to form nanocrystals with magic numbers. 'Hot' nanocrystals with magic numbers undergo losses of monomers and dimers but with much reduced probability.

We assume a dominance of monomer alkali halide evaporation as well as the steady state approximation in the number of any one of the nanocrystals, e. g. $[Rb_kK_{14-k}I_{13}]^+$ which we call $N_{k,13}$. This nanocrystal is formed by nucleation with a rate of $K_{13}N_k^{isom}$, and from the evaporation of a KI molecule from the $M_kI_{14}^+$ nanocrystal with a rate of $\rho_{14}N_{k,14}$, where ρ_{14} is the rate constant and $N_{k,14}$ is the steady state number of the $[Rb_kK_{15-k}I_{14}]^+$ nanocrystal. The $[Rb_kK_{14-k}I_{13}]^+$ nanocrystal would give the $[Rb_kK_{13-k}I_{12}]^+$ nanocrystal upon the evaporation of a KI molecule.

With the above kinetic scheme, one obtains for the steady state number of the $M_kI_{13}^+$ nanocrystal, $N_{k,13}$, the following expression:

$$N_{k,13} = \sum_{j=13}^{14} K_j \, N_{k,j}^{isom} / \rho_{k,13} \quad \text{----------} \quad (8)$$

Due to the fact that K_j falls rapidly in value with j, as seen from eq. (5), j=13 will be the dominant term in the sum of eq. (8).

If the sensitivity of the detector is the same for all the mixed nanocrystals, the predicted intensity of the peak corresponding to the k,13 nanocrystal is given by

$$I_{k,13} \approx K_{13} N_{k,13}^{isom} / \rho_{k,13} \quad \text{----------} \quad (9)$$

The predicted intensity from equation (9) would account for the observation in Fig. 2, if $\rho_{k,13}$ is independent of k, implying that the rate constant of evaporation from any of the magic mixed nanocrystals is insensitive to their composition.

For a certain channel of evaporation , e.g. the loss of KI, the activation energy, which determines the value of the rate constant (ρ), is determined by the difference between the internal energies of the $[Rb_kK_{14-k}I_{13}]^+$ and the sum of the energies of KI + $[Rb_kK_{13-k}I_{12}]^+$. This is only true in the absence of a reverse activation energy, which is found to be the case for the evaporation of CsI from $[Cs_mI_{m-1}]^+$ clusters[1]. For $\rho_{k,13}$ to be independent of k, one is thus forced to conclude that the internal energies of the $[Rb_nK_{14-n}I_{13}]^+$ nanocrystals are similar and insensitive to their composition, i.e. to the value of n. In order to test this conclusion, we have carried out in the next section a Monte Carlo simulation of the internal energies of these clusters for n= 0 to 14.

V. A. Computational Method

The Metropolis Monte Carlo method[43] was used to minimize the total energy of mixed nanocrystals through optimization of their geometry. We used the polarizable-ion model[29, 33-35, 37] which includes the deformation

of the electron density as atoms come close to one another. Even though there is a substantial free surface present in these clusters, the covalent bonding forces are absent, and these alkali halides are ionically bound[25]. Thus, we can use very simple model potentials to study their binding energies theoretically[25].

The binding energies of the mixed nanocrystals were calculated by minimizing the total potential energy written as sum of the pairwise coulomb interaction, the short-range Born-Mayer repulsive interaction due to the overlap of electron clouds on two nearest neighbors, charge-dipole interactions, dipole-dipole interactions, and self-energy of the dipoles[33]. In the Born-Mayer repulsive term, an effective radius is used which accounts for the deformation of the electron shells at small distances[24]. The parameters used in our calculations, e.g. polarizabilities, and effective radii, were taken from Welch[24] et. al. and Born[38]. In the Born-Mayer potential, the interactions for the like-charges have not been considered. These interactions are negligible since the overlap of the repulsive electron densities among them is minimized due to their relatively large separations.

In the calculation, we start with the bond distances of $(KI)_2$ and/or $(RbI)_2$ as the initial bond distances between the ions in our nanocrystals[29, 30]. The nanocrystal configuration is allowed to relax by randomly moving the three independent coordinates of each atom in the nanocrystal. After each move, a change in the total energy (ΔE) between the initial and final structure is calculated. If ΔE is negative or zero, the new structure is accepted. otherwise, it is accepted with a probability of

$\exp(-\Delta E/kT)$[33-35]. The temperature is lowered gradually for the calculation of the ground state energy. About 200000 (or more) sweeps are performed in order to increase the probability of reaching a global minimum[34]. The computer code for our calculation was modified from that of Li[28]. The results of our calculations for the binding energies of all the different nanocrystals are given in Table 1.

V. B. Computational Results

The results of our calculation for the total binding energies are given in Table 1. A slight monotonic increase in the calculated values of the binding energies is obtained as the number of Rb ions in the mixed nanocrystal increases. However, the difference in the energies is smaller than the inherent error in our calculations. Thus, within the limit of the errors in our calculations, we can conclude that the internal energies of the mixed nanocrystals of the type $[Rb_nK_{14-n}I_{13}]^+$ (n=0-14) are rather insensitive to their composition.

The vibrational frequencies of the monomeric KI is larger than that for RbI (186.53 cm^{-1}, and 138.511 cm-1, respectively)[44] in the gas phase. The effect of this would come in the zero point energy contributions to the binding energies of the nanocrystals of $[Rb_nK_{14-n}I_{13}]^+$ (n=0-14). This is expected to decrease the calculated energy difference between nanocrystals.

Furthermore, in our calculation of the binding energies, we considered only a small number of the possible isomers for each of the

$[Rb_nK_{14-n}I_{13}]^+$ (n=0-14) nanocrystals. There are many isomers for any one of the nanocrystals and many of these isomers would be present significantly at the high temperatures of our experiment, which is ~ 750 K. All these factors suggest that the small calculated difference in the internal energies of the nanocrystals is not significant. One can then conclude that these mixed nanocrystals have comparable energies. This conclusion is not at all surprising in the light of the fact that the lattice energy[22] of bulk KI (-149.9kcal/mol) is comparable to that of RbI(-144.9 kcal/mol).

Acknowledgment

The authors wish to thank C. K. Fagerquist for his instrumental assistance. The financial support of the Office of Naval Research (Contract N00014-89-J-1350) is greatly appreciated.

References

1. Hwang, H. J.; Sensherma, D. K. ; El-Sayed, M. A. *Chem. Phys. Lett.* 1989, 160, 243.

2. Honda, F.; Lancaster, G. M. ; Fukuda, Y.; Rabalais, J. W. *J. Chem. Phys.* 1978, 69, 4931.

3. Li, X. ; Whetten, R. L. *J. Chem. Phys.* 1993, 98, 6170.

4. Beck, R. D.; St. John, P. M. ; Homer, M. L.; Whetten, R. L. *Chem. Phys. Lett.* 1991, 187, 122.

5. Beck, R. D. ; St. John, P. ; Homer, M. L. , Whetten, R. L. *Science* 1991, 253, 879.

6. Luo, J.; Landman, U.; Jortner, J. in *Physics and Chemistry of Small Clusters* Jena, P.; Rao, B. K.; Khanna, S. N. Eds.; Plenum Publishing Corporation, 1987, P. 200.

7. Galli, G.; Andreoni, W.; Tosi, M. P. *Phys. Rev. A* 1986, 34, 3580.

8. Giraud-Girard, J.; Maynau, D. *Z. Phys. D* 1992, 34, 3580.

9. Drewello, T.; Herzschuh, R.; Stach, J. *Z. Phys. D* 1993, 28,339.

10. Martin, T. P. *Ber. Bunsenges. Phys. Chem.* 1984,88,300.

11. Martin, T. P. *J. Chem. Phys.* 1978, 69, 2036.

12. Diefenbach, J.; Martin T. P. *J. Chem. Phys.* 1985, 83, 2238.

13. Diefenbach, J.; Martin T. P. *J. Chem. Phys.* 1985,83, 4585.

14. Ahlrichs, R.; Ochsenfeld, C. *Ber. Bunsenges. Phys. Chem.* 1992, 96, 1287.

15. Philips, N. G.; Conover, C. W. S.; Bloomfield, L. A. *J. Chem. Phys.* 1991, 94, 4980.

16. Campana, J. E.; Barlak, T. M. ; Wyatt, J. R. ; Colton, R. J. ; DeCorpo, J. J. *Phys. Rev. Lett.* 1981, 47, 1046.

17. Dunlap, B. I. *J. Chem. Phys.* 1986, 84, 5611.

18. Campana, J. E.; Dunlap, B. I. *Int. J. Mass Spectrom. Ion Processes* 1984, 57, 103.

19. Barlak, T. M. ; Wyatt, J. R. ; Colton, R. J. ; DeCorpo, J. J. ; Campana, J. E. *J. Am. Chem. Soc.* 1982, 104,1212.

20. Barlak, T. M. ; Wyatt, J. R. ; Colton, R. J. ; DeCorpo, J. J. ; Campana, J. E. *J. Phys. Chem.* 1983, 87, 3441.

21. Hwang, H. J.; Sensherma, D. K. ; El-Sayed, M. A. *J. Phys. Chem.* 1989,93, 5012.

22. Hwang, H. J.; Sensherma, D. K. ; El-Sayed, M. A. *Phys. Rev. Lett.* 1990,64, 808.

23. Welch, D. O.; Lazareth, O. W.; Dienes, D. J.; Hatcher, R. D. *J. Chem. Phys.* 1978, 68, 2159.

24. Welch, D. O.; Lazareth, O. W.; Dienes, D. J.; Hatcher, R. D. *J. Chem. Phys.* 1976, 64, 835.

25. Bloomfield, L. A.; Conover, C. W. S.; Yang, Y. A.; Twu, Y. J.; Phillips, N. J. *Z. Phys. D* 1991, 20, 93.

26. Pflaum, R.; Pfau, P.; Sattler, K.; Recknagel, E. *Surface Sci.* 1985, 156, 165.

27. Phillips, J. C. in *Physics and Chemistry of Small Clusters* Jena, P.; Rao, B. K.; Khanna, S. N. Eds.; Plenum Publishing Corporation, 1987, P. 249.

28. Li, X. PhD. Dissertation, University of California, Los Angeles, 1993.

29. Ramondo, F.; Bencivenni, L. *J. Mol. Struct.* 1989, 193, 203.

30. Ramondo, F.; Bencivenni, L. *J. Mol. Struct.* 1989, 192, 73.

31. Ens, W. ; Beavis, R. ; Standing, K. G. *Phys. Rev. Lett.* 1983, 50, 27.

32. Morgan, T. G.; Rabrenovic, M.; Harris, F. M.; Beynon, J. H. *Org. Mass Spec.* 1984, 19, 315.

33. Martin, T. P. *Phys. Rep.* 1983, 95, 167.

34. Wille, L. T. *Chem. Phys. Lett.* 1987, 133, 405.

35. Kirkpatrick, S.; Gellat, C. D.; Vecci, M. P. *Science* 1983, 220, 671.

36. Cooks, R. G.; Beynon, J. H.; Caprioli, R. M.; Lester, G. R. *Metastable Ions*, Elsevier, Amsterdam, 1973, P.60.

37. Rittner, E. S. *J. Chem. Phys.* 1951, 19, 1030.

38. Born, M.; Huang, K. Dynamical Theory of Crystal Lattices, Oxford University Press, London, 1954.

39. Twu, Y. J.; Conover, C. W. S.; Yang, Y. A.; Bloomfield, L. A. Phys. Rev. B 1990, 42, 5306.

40. Bucher, J. P.; Bloomfield, L. A. Z. Phys. D 1991, 20, 361.

41. Fagerquist, C. K.; Sensherma, D. K. ; Ahmadi, T. S.; El-Sayed, M. A. *J. Phys. Chem.* 1993, 97, 6598.

42. Metropolis, N.; Rosenbluth, M.; Rosenbluth, A.; Teller, E. *J. Chem. Phys.* 1953, 21, 1087.

43. Blander, M. in Alkali Halide Vapors Davidovits, P.; McFadden, D. L. Eds.; Academic Press, New York, 1979, p.8.

* Ion Tech Ltd, Teddington, Middlesex, UK.

Table 1 The calculated binding energies of the $[Rb_nK_{14-n}I_{13}]^+$ (n=0-14) nanocrystals as obtained through Monte Carlo Simulation Annealing.

n in the $[Rb_nK_{14-n}I_{13}]^+$	Binding Energy (eV)
0	-80.52±1.8
1	-80.65±3.62*
2	-80.54±3.60*
3	-80.10±3.58*
4	-79.76±3.57
6	-79.78±3.55*
7	-79.53±3.55*
8	-78.33±3.51*
9	-78.34±3.51
10	-78.26±3.50
11	-78.06±3.44
12	-78.37±3.45*
13	-78.59±3.60*
14	-77.96±3.50*
Average Energy	-79.23±3.50

* average of more than one isomer.

Figure Captions

Figure 1 The observed mass spectrum resulting from the sputtering of a solid mixture of KI and RbI. Marked are the peaks corresponding to the mixed magic nanocrystals $[Rb_nK_{14-n}I_{13}]^+$ for n = 0, 1, ... , 14 .

Figure 2 The calculated relative intensity of kth mixed nanocrystal (relative to all the nanocrystals formed) as calculated from the observed intensities of the fifteen peaks of the nanocrystals of $[Rb_nK_{14-n}I_{13}]^+$ for n= 0-14.

Figure 3 The predicted dependence of the relative number of isomers of the mixed nanocrystals on their composition(i.e. the number of KI and RbI molecules) . The mixed nanocrystal having equal number of KI and RbI (n=7) has the largest relative number of isomers.

Figure 1

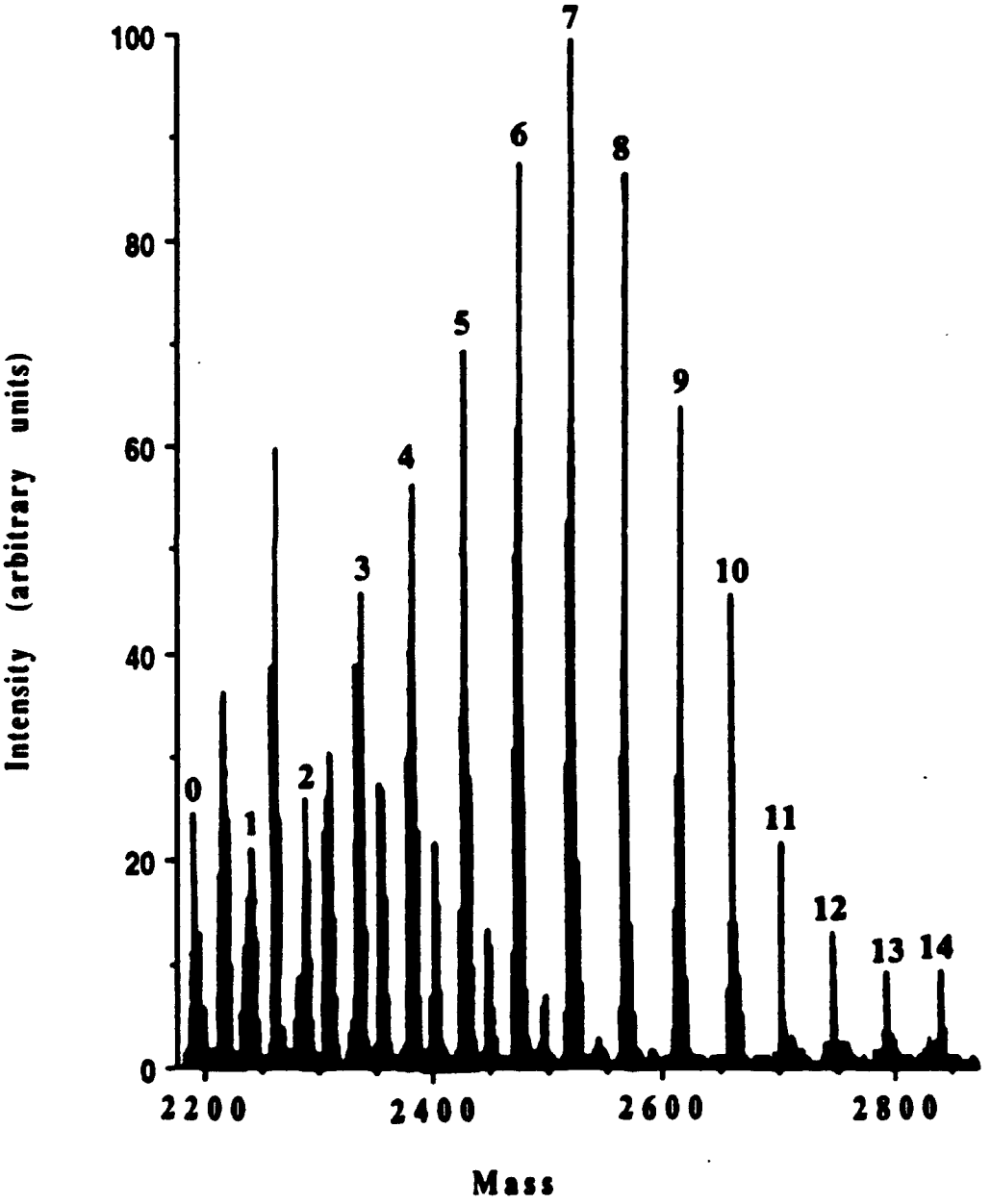
Intensity (arbitrary units)
100
80
60
40
20
0
0
1
2
3
4
5
6
7
8
9
10
11
12
13
14
2200
2400
2600
2800
Mass

Figure 2

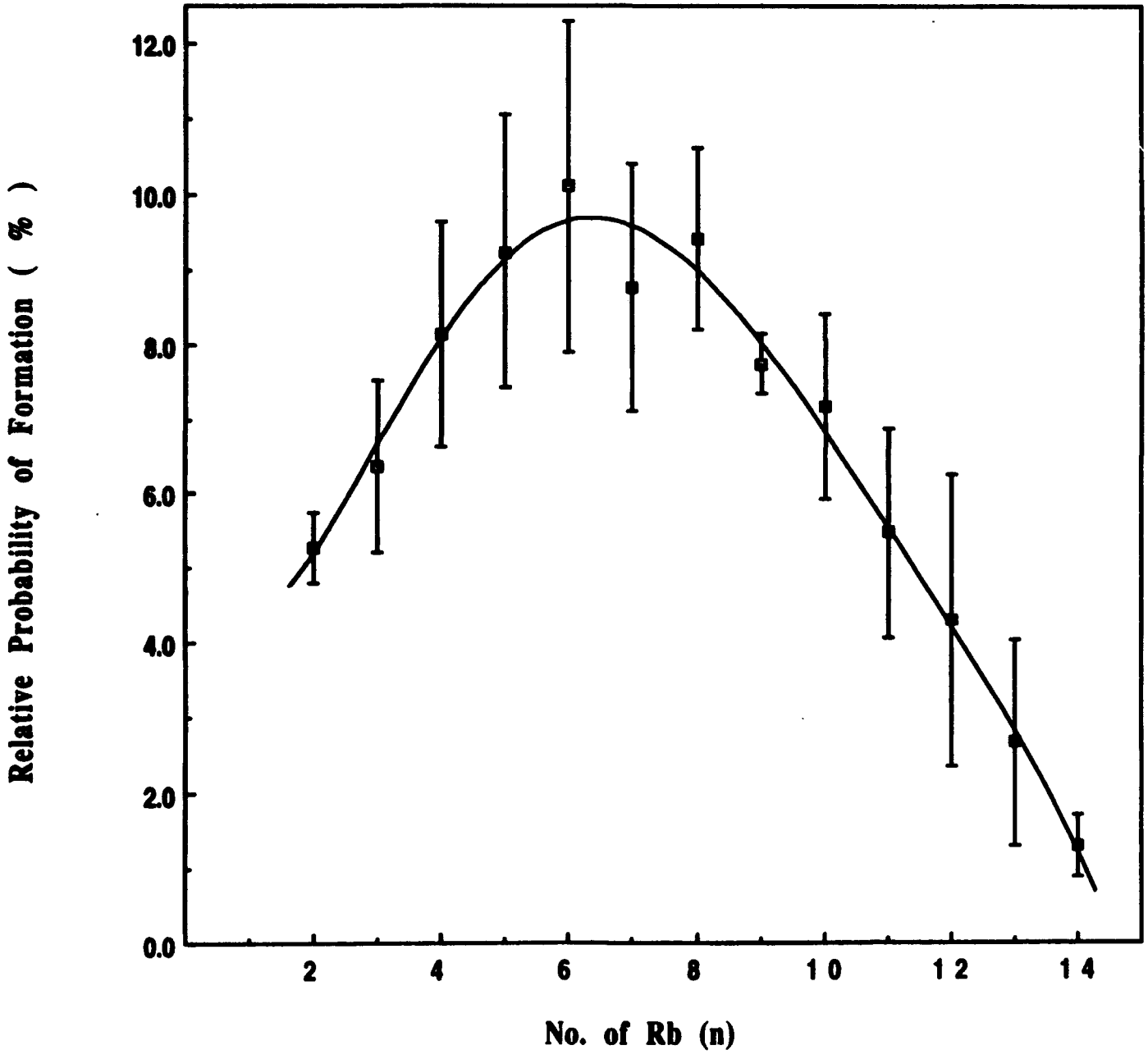
Relative Probability of Formation (%)
12.0
10.0
8.0
6.0
4.0
2.0
0.0
2
4
6
8
10
12
14
No. of Rb (n)

Figure 3